Optimum Generation Control in Wind Parks When Carrying Out System Operator Requests

Rogério G. de Almeida, Edgardo D. Castronuovo, *Member, IEEE*, and J. A. Peças Lopes, *Senior Member, IEEE*

***Abstract*—This paper proposes an optimized dispatch control strategy for active and reactive powers delivered by a doubly fed induction generator in a wind park. In this control approach, wind turbines are supposed to operate over a deloaded maximum power extraction curve and will respond to a supervisory wind farm control after a request from a system operator for adjusting the outputs of the wind park. The definition of the active and reactive powers operating points, for each wind turbine, is defined from an optimization algorithm that uses the primal-dual predictor corrector interior point method. The control strategy used at the wind generator level exploits a combination of pitch control and control of the static converters to adjust the rotor speed for the required operation points. A small wind park is used to illustrate the effectiveness of the developed approach.**

***Index Terms*—Active and reactive power dispatch, control systems, nonlinear programming, optimization strategies, wind generators.**

I. Introduction

NOWADAYS, wind parks are more and more required to provide control capabilities regarding active and reactive power outputs either because of their participation in electricity markets or because of the need of the grid to be operated under desired security levels. Under this scenario, these generation facilities are expected to be able to control their active and reactive power outputs. The availability of these control capabilities in wind generators results from the use of advanced electronic converters that, together with adequate control strategies, enable the implementation of the controllability requirements.

At the same time, the large increase of the penetration of wind generation in power systems is leading to the development of updated grid codes that are imposing a set of technical requirements to wind generation, with a major concern on the system security issues.

Among the different wind energy conversion (WEC) systems used [1], [2], double fed induction wind generators (DFIWGs) are units capable of providing the required capabilities, without the need of great costs on the power electronics hardware. In general, DFIWGs are operated with variable rotational speed, extracting maximum power from the wind turbine for a given wind speed. A great variety of control strategies can be used in the operation of DFIWG and has been described in several works [3]–[7].

Independently of the type of wind energy conversion systems used, these units are to be operated in wind parks or clusters of wind parks for which the grid requirements apply, which means that a control on active and reactive powers output of the wind farms needs to be addressed in a hierarchical manner [8]. Internal optimization procedures to allocate to the generating units in a cluster the adequate power output values are therefore needed.

This paper tackles two issues:

1) implementation of an optimization strategy to be adopted at a supervisory wind farm control (SWFC) level with the objective of assuring that the wind park active and reactive power outputs comply with the requests defined by system operators.
2) development of a control strategy for DFIWG to allow for their response to set points for active and reactive power outputs received from the SWFC.

The optimization procedure defines set points that correspond to the allocation of the active and reactive powers in each wind generator and allows the park output to follow closely the system operator requests, taking into account the wind park internal losses and the availability of the wind resource. The solution of the optimization problem uses a primal-dual predictor corrector interior point method.

The implementation of this control approach in the DFIWG required the inclusion of a secondary active power control loop. The DFIWGs used are already able to provide primary frequency control capabilities.

In order to be able to provide some primary frequency capability response, wind turbines (WTs) are supposed to operate on a deloaded maximum power extraction curve, for a given wind speed, in which the pitch control is used simultaneously with static converters to adjust the wind turbine rotor speed (referred to as the generator side).

In order to evaluate the effectiveness of the developed control approach, a small wind farm connected to an infinite bus bar is used in this paper for testing purposes. Results from the optimization approach developed and the dynamic response of the wind turbines are discussed.

II. Structure of the Wind Farm

In general, a wind farm is made of wind generators connected to each other in a cascade manner, forming feeders that leave the

Manuscript received June 2, 2005; revised October 6, 2005. This work was supported by Fundação para a Ciência e Tecnologia de Portugal (FCT) under the DIPTUNE POCTI/41614/ESE/2001 project. Paper no. TPWRS-00340-2005.

R. G. de Almeida and E. D. Castronuovo are with the Instituto de Engenharia de Sistemas e Computadores do Porto, 4200-465 Porto, Portugal (e-mail: ralmeida@inescporto.pt; castronuovo@ieee.org).

J. A. Peças Lopes is with the Instituto de Engenharia de Sistemas e Computadores do Porto and Faculdade de Engenharia da Universidade do Porto, 4200-465 Porto, Portugal (e-mail: jpl@fe.up.pt).

Digital Object Identifier 10.1109/TPWRS.2005.861996

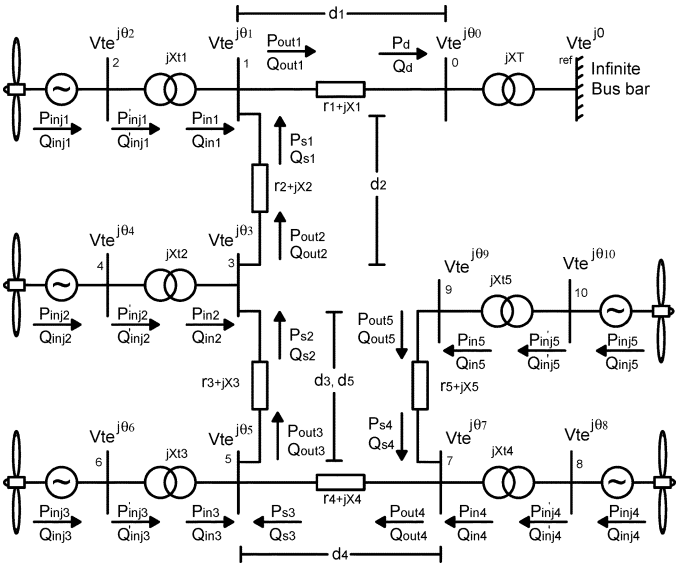

Fig. 1. Wind farm configuration.

main substation, as illustrated in Fig. 1 for the small wind park used in this paper.

Part of the total active and reactive power delivered by the wind generators is lost inside the wind park network. If a certain set point regarding active and or reactive power is requested to the wind park output, it is important to determine what should be the active and reactive power generation levels of each unit such that the wind park is able to meet the system operator demand. Such determination is performed at the SWFC level. The next sections describe the approach developed to allocate these generation amounts (that define set points for the wind generators) and the adjustments in the control loops of the DFIWG for being able to respond to these requests.

A. Optimization Problem

The proposed method aims to obtain a minimum deviation between the total active and reactive powers delivered by the wind farm to the grid as required by the system operator. In this optimization problem, two cases are studied:

a) minimum active and reactive wind park output power deviations regarding the system operator request;
b) minimum active and reactive power deviations of the wind park output regarding the system operator request, considering also the minimization of the active power losses in order to exploit the available primary wind resource in the best way. These losses are a function of the wind park internal electrical network branch characteristics.

According to Fig. 1, the following optimization problem for each scenario can be solved:

$$Min\left\{p_1(P_d - P_{total})^2 + p_2(Q_d - Q_{total})^2 + \ldots \right. \\ \left. p_3\left[(P_{out_1} - P_d)^2 + \sum_{i=2}^{n}\left(P_{out_i} - P_{S_{i-1}}\right)^2\right]\right\} \quad (1)$$

s.t.

$$P_{out_i}(V,\theta) = P_{in_i}(V,\theta) + P_{S_i}(V,\theta) \quad (2)$$

$$Q_{out_i}(V,\theta) = Q_{in_i}(V,\theta) + Q_{S_i}(V,\theta) \quad (3)$$

$$P_{inj_i} = P'_{inj_i}(V,\theta) \quad (4)$$

$$Q_{inj_i} = Q'_{inj_i}(V,\theta) \quad (5)$$

$$P_{\min_i} \le P_{inj_i} \le P_{o_i} \quad (6)$$

$$Q_i^m \le Q_{inj_i} \le Q_i^M \quad (7)$$

$$V_i^m \le V_i \le V_i^M \quad (8)$$

$$\theta^m \le \theta_i \le \theta^M \qquad i = 1, \ldots, n \quad (9)$$

where the vectors $\boldsymbol{P}_{out}$, $\boldsymbol{P}_{in}$, $\boldsymbol{P}_S$, and $\boldsymbol{P}'_{inj}$ as well as $\boldsymbol{Q}_{out}$, $\boldsymbol{Q}_{in}$, $\boldsymbol{Q}_S$, and $\boldsymbol{Q}'_{inj}$ represent the active and reactive powers flowing in the branches of the wind park, according to Fig. 1, being these power flows defined from well-known load flow equations between two bus bars as described in detail in [9], with $\boldsymbol{V}$ and θ being the vectors of the voltages and phase angles of the network nodes. P_d and Q_d are the total active and reactive wind park power outputs, defined by the same load flow equations.

The elements of the vectors $\boldsymbol{P}_{inj}$ and $\boldsymbol{Q}_{inj}$ are the active and reactive powers injected by each WT into the wind park grid, to be determined by the optimization algorithm; P_{total} and Q_{total} are the active and reactive output powers requested by the system operator; p_1, p_2, and p_3 are weight factors, defined according to the simulation scenario; and n is the number of WTs in the wind farm.

The objective function defined in (1) contains three parts: the first one aims to decrease in a quadratic form the deviation between the total active power output of the wind farm and the system operator requests; the second one seeks to reduce in a quadratic form the deviation between the total reactive power output and the required reactive power requested by the system operator; and the third one seeks the quadratic decrease of the active power losses. The losses considered in (1) are the wind farm internal ones, related with the active power losses in the transformers and lines inside the wind farm. The three parts of the objective function are linked through weight factors, representing the influence of each term of (1) in the situation under analysis. In case *a*, $p_1 = 1$, $p_2 = 0.5$, and $p_3 = 0$; in case *b*, $\text{p1} = 1$, $p_2 = 0.5$, and $p_3 = 0.5$. It must be stressed that other objective functions can be easily considered in the optimization problem, as a function of the particular interest of the wind park developer. Among others, the following alternative objective functions can be considered: minimization of reactive power losses, minimization of deviations from a pre-specified reserve margin, or others.

The operational limits of the individual wind generators are shown in (6)–(9), where the maximum active power that each turbine can produce (P_{oi}) according to (6) depends on the available wind power in the WT and from a pre-defined active power curve adopted by the DFIWG active power control loop. The minimum deloaded active power (P_{min}) is a function of the P_{oi}, and it is discussed next.

The reactive power generation limits for each WT are defined in (7) and are assumed in a range of $[-0.0028; 0.0028]$ in p.u. (in the system base).

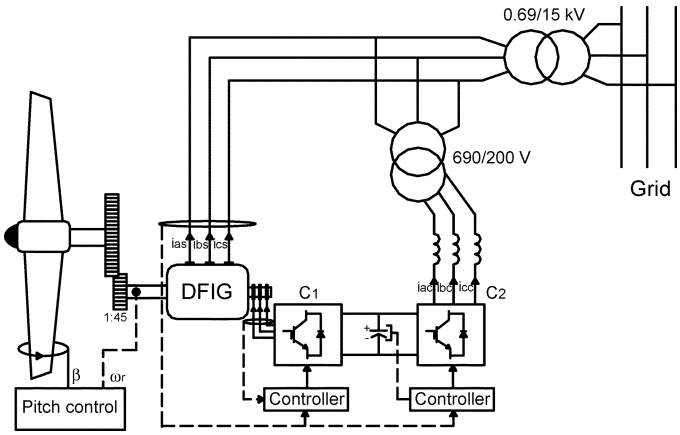

Fig. 2. General control scheme of DFIG, converters, and controllers.

Restrictions (8) express the limits in the voltage control imposed to all the buses according to the protection relay settings. An allowable range of [0.9; 1.1] was adopted in this paper.

Finally, the limits of bus angles are defined in (9) and are assumed in a range of $[-\pi;\pi]$ for the purpose of the optimization search procedure.

In some wind parks, the reactive power management system uses shunt capacitive or inductive elements $y_{\rm shi}$ that can be inserted or removed. If these elements are installed in parallel with the wind generators, which is the usual situation, a post-processing stage is needed to evaluate the contribution that the available shunts can provide for the $\boldsymbol{Q}_{inj}$ injected reactive powers, determined from the optimization procedure. For that purpose, the magnitude of the voltages in each turbine bus is maintained from the solution of the optimization problem. The amount of reactive power each ith wind generator should then produce is given by $Q_{\rm i} = Q_{\rm inji} - V_{\rm i}^2 y_{\rm shi}$. When these shunt elements have several steps, the number of capacitive or inductive elements that should be connected should assure that the condition $|V_{\rm i}^2 y_{\rm shi}| \leq |Q_{\rm inji}|$ is verified.

The optimization problem defined in (1)–(9) is characterized by a nonlinear problem, being solved in this research by using a predictor-corrector primal-dual interior point algorithm [10].

The determination of these active and reactive power generation levels leads to the definition of setting points to be sent to the control loops of each generator (DFIWG in this case).

B. Doubly Fed Induction Wind Generator Control

A full description of the DFIWG mathematical model used in this paper is given in more detailed way in [7]. Fig. 2 depicts the general scheme of the DFIWG, converters, and controllers adopted in this paper.

The control strategy used to control the rotor-side converter, modeled as a voltage source, consists of a $d-q$ voltage regulator. To accomplish the active/reactive power control, the rotor-side converter operates in a $d-q$ reference frame, controlling both active and reactive power outputs through v_{qr} and v_{dr} components, obtained from two separate sets of PI controllers. Additional information about this control scheme is presented in [3]. The PI controllers involve a cascade structure, where the outside PI blocks are used to regulate the reference rotor currents (i_{qref} and i_{dref}), and the inner side PI blocks are used to regulate the v_{qr} and v_{dr} components, respectively.

Through the rotor-side active power control loop, the wind turbine can be driven to operate with maximum power once the reference active power input of the control system is set from a wind turbine deloaded optimal power curve, as described in the next section.

On the other hand, the grid-side converter C2 is designed to control only the dc link voltage, taking into account the balance of the active power between the rotor and the grid. The control algorithm implemented to control converter C2 is based on concepts of instantaneous active and reactive powers theory, as explained in full detail in [11].

C. Deloaded Optimal Operating Point of Variable-Speed Wind Turbine

The optimum mechanical power obtained from a given wind speed is defined by the following equation:

$$P_{opt} = \frac{1}{2}\rho C_{p_{opt}}(\lambda_{opt},\beta)AU_w^3. \tag{10}$$

With $C_{p_{opt}}$ being the optimal power coefficient of the wind turbine for a given wind speed, A (m^2) is the effective area covered by the turbine blades, U_w $(\mathrm{m/s})$ is the wind speed, and ρ $(\mathrm{Kg/m}^3)$ is the air density.

The calculation of the optimal power coefficient $C_{p_{opt}}$ can be obtained from the following function, as suggested in [2]:

$$C_{p_{opt}}(\lambda_{opt},\beta) = 0.22\left(\frac{116}{\lambda_i} - 0.4\beta - 5\right)e^{\frac{-12.5}{\lambda_i}} \tag{11}$$

$$\frac{1}{\lambda_i} = \frac{1}{\lambda_{opt}+0.08\beta} - \frac{0.035}{\beta^3+1}. \tag{12}$$

With the optimal tip speed ratio defined as

$$\lambda_{opt} = \frac{\omega_{t_{opt}}R}{U_w} \tag{13}$$

where R (m) is the blade radius, and $\omega_{t_{op}}$ is the optimal wind turbine rotor speed (rad_mec/s) for a given wind speed.

From (10) and (13), an optimum (maximum) power value—P_{opt}—can be obtained as a function of the shaft speed, referred to the generator side of the gearbox as follows:

$$\mathrm{P}_{opt} = k_{opt}\omega_r^3 \tag{14}$$

where

$$k_{opt} = \left(\frac{1}{2}\right)\rho\left(\frac{C_{p_{opt}}}{\lambda_{opt}^3}\right)\pi R^5 \tag{15}$$

$$\omega_r = \left(\frac{p}{2}\right)G\omega_t \tag{16}$$

with p being the number of poles of the generator and G the transmission ratio of the gearbox.

From (14), the wind turbine pre-defined optimum power extraction curve can be established for a given k_{opt} associated to an optimum fixed blade angle. However, in order to make possible the increase or decrease of the reference active power input (P_{del} in Fig. 6) of the DFIWG active power loop, for a

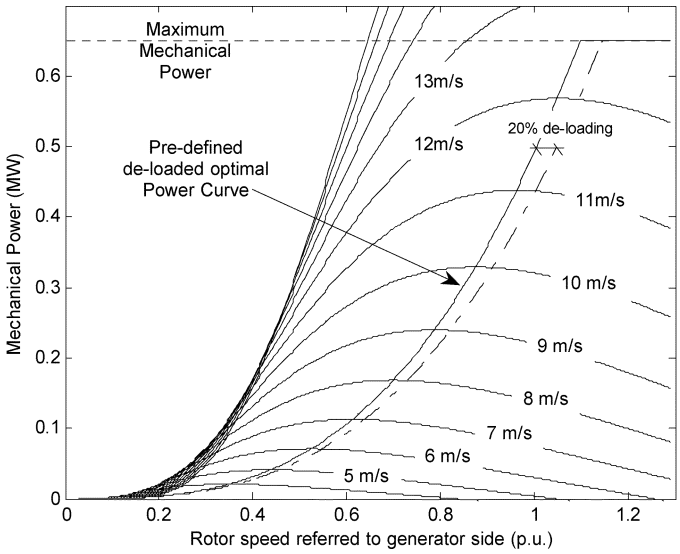

Fig. 3. Optimum power extraction and deloaded power curves.

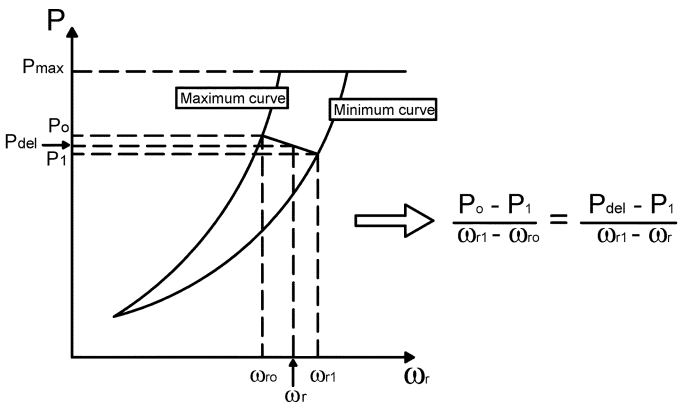

Fig. 4. Schematic diagram of deloaded active power.

given wind speed, the wind turbine must operate with deloaded power curves, which are pre-defined according to the requested active power output imposed by wind park supervisory control. In other words, if the individual active power request, defined by the optimization algorithm running in the SWFC, exceeds the deloaded optimal power curve range, where the DFIWG is operating, a search procedure was integrated into optimization algorithm and used to define a new deloaded active power curve for each WT in order to be able to respond to the SWFC set point. In this paper, a pre-defined deload of 20% was adopted, as shown in Fig. 3.

As observed in Figs. 3 and 4, the reference for active power control loop is considered to be situated between the maximum and the 20% deloaded power curve, for a given wind speed. In this way, a line equation can be used to describe the changes around ω_r (see Fig. 4). This relationship is described as follows.

From Fig. 4, the reference active power P_{del} can be defined as

$$P_{del} = P_1 + \frac{P_o - P_1}{\omega_{r1} - \omega_{ro}}(\omega_{r1} - \omega_r) \tag{17}$$

where P_o and P_1 are the maximum and deloaded active powers for a given wind speed, respectively, with ω_{ro} and ω_{r1} being the minimum and maximum rotor speeds referred to the generator side. However, the relationship between P_o and P_1 is defined as

$$P_1 = k_{del} P_o \tag{18}$$

where

$$k_{del} = \left(1 - \frac{\%_{\text{de-loading}}}{100}\right) \tag{19}$$

$$P_1 = k_{op1}\omega_{r1}^3 \tag{20}$$

$$P_o = k_{opo}\omega_{ro}^3 \tag{21}$$

with k_{opo} and k_{op1} being the optimum constants defined as described in (15) for both maximum and minimum power curves, respectively.

From (19)–(21), the maximum and minimum rotor speeds can be given as

$$\omega_{r1} = \left(\frac{k_{del}k_{opo}}{k_{op1}}\right)^{\frac{1}{3}} \omega_{r0}. \tag{22}$$

So, (18) can be rewritten as

$$P_{del} = \left\{ \frac{(\omega_r - \omega_{ro})k_{del} + \left[\left(\frac{k_{del}k_{opo}}{k_{op1}}\right)^{\frac{1}{3}} \omega_{ro} - \omega_r\right]}{\left[\left(\frac{k_{del}k_{opo}}{k_{op1}}\right)^{\frac{1}{3}} - 1\right]\omega_{ro}} \right\} P_o. \tag{23}$$

In (23), P_{del} basically becomes dependent on rotor speed ω_r, assuming that P_o and ω_{ro} are previously known for a given wind speed of the adopted deloaded active power curve.

D. Pitch Control Strategy

Pitch control is used simultaneously with static converters adjusting the rotor speed referred to generator side according to the deloaded maximum power curve. For wind speeds below maximum rated speed (as described in Fig. 3), the input reference for active power that feeds the DFIG active power loop follows (23), and the input reference for rotor speed to the pitch control loop is defined as

$$\omega_{ref} = \frac{P_{del}}{T_{mec}}. \tag{24}$$

Nevertheless, for wind speeds larger than maximum rated speed, the blade pitch regulation dominates the control and limits the energy captured from the turbine. In this case, the pitch control will control the rotor speed and will operate until the wind cut-off speed limit is reached (1.2 p.u.). The speed reference for pitch control is defined as

$$\omega_{ref} = \frac{P_{\max}}{T_{mec}}. \tag{25}$$

The implementation at the individual generator level of the active power set points received from the SWFC can be

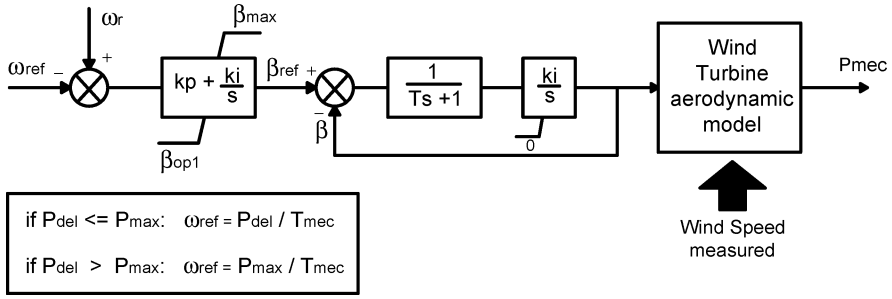

Fig. 5. Pitch control schematic diagram.

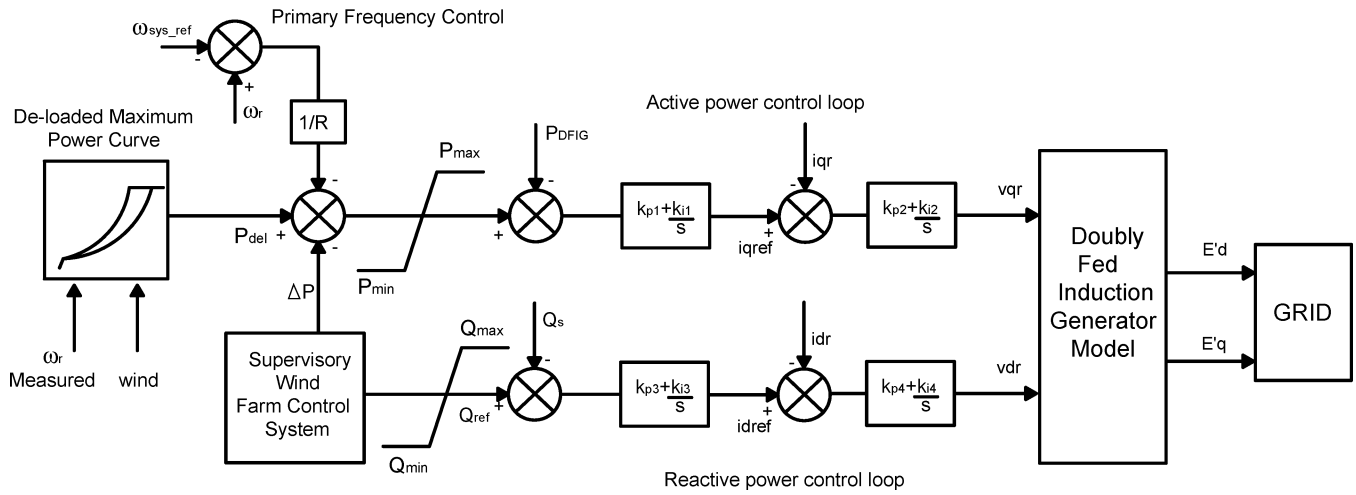

Fig. 6. Full control approach adopted for rotor-side converter.

performed by adjusting the pitch angle of the turbines, requiring, however, a different control sequence that involves the determination of the pitch angle to be used, generally through a mechanical characteristics look-up table, enabling then the identification of a reference speed (obtained from the corresponding maximum extraction power curve) that would be used in a active power rotor control loop of the type described in [8]. Through the use of the combined rotor side electronic/pitch control approach described in this paper, larger control flexibility is achieved, avoiding the use of the look-up table mentioned before, since the active power set point received from the SWFC leads to a new reference active power to which corresponds a new reference in rotor speed (obtained from the deloaded curve), used afterwards by the pitch control, described in Fig. 5, to find the new pitch angle.

The pitch control schematic diagram and the full control approach adopted for the rotor side converter are shown in Figs. 5 and 6, respectively. Fig. 6 provides a general overview of the control loops used to control the DFIWG.

III. Simulation Results

To test the proposed methodology, a small wind farm with five DFIWG, as illustrated in Fig. 1, was used. The line and transformer parameters are described in Table I (values are in p.u. referred to as the system base). The full wind conversion system parameters are presented in the Appendix.

The optimization scenarios presented in this section involve the approach described for cases *a* and *b*. For both cases, an equal wind speed has been adopted in all WT. All wind turbines were supposed to operate with the same deloaded maximum power extraction curve (see Fig. 3) with a 20% deloading. Both simulation scenarios are described next.

TABLE I
Line Parameters

Line impedance p.u.		Dist. (Km)	X_t (pu)
Z_1	0.7690+j0.0603	$d_1 = 1.200$	6.667
Z_2	0.1986+j0.0156	$d_2 = 0.310$	6.667
Z_3	0.1986+j0.0516	$d_3 = 0.310$	6.667
Z_4	0.1986+j0.0516	$d_4 = 0.310$	6.667
Z_5	0.1986+j0.0516	$d_5 = 0.310$	6.667

(X_t is the wind generator stator transformer reactance)

A. Cases a and b Considering Equal Wind Speed

In this scenario, it will be assumed that all wind turbines are operating with wind speed equal to 12 m/s, corresponding to an injecting maximum active power equal to 0.005 685 p.u. (0.5685 MW). In this case, the total active power injected by the wind farm into the grid corresponds to 0.0285 (2.85 MW). On the other hand, it was assumed that before running the optimization allocation process, all WT were injecting 0.0027 p.u. (0.27 MVAr) of reactive power corresponding to a $tang\varphi = 0.4$ capacitive.

TABLE II
OPTIMIZATION RESULTS

Wind Gen. at bus bar	*Case a*		*Case b*	
	Injected. Act. Power (MW)	Injected. React. Power (MVAr)	Injected. Act. Power (MW)	Injected. React. Power (MVAr)
02	0.5142	0.2097	0.5685	0.2800
04	0.5164	0.2458	0.5685	0.2800
06	0.5144	0.2479	0.5223	0.1813
08	0.5140	0.2479	0.4550	0.2404
10	0.5139	0.2479	0.4548	0.2165
Total	2.5729	1.1992	2.5690	1.1982
Active Power Losses	Total = 46.157 kW		Total = 44.446 kW	
Total Delivered by Wind Farm to the Grid	MW	MVAr	MW	MVAr
	2.5	1.0	2.4981	0.9983

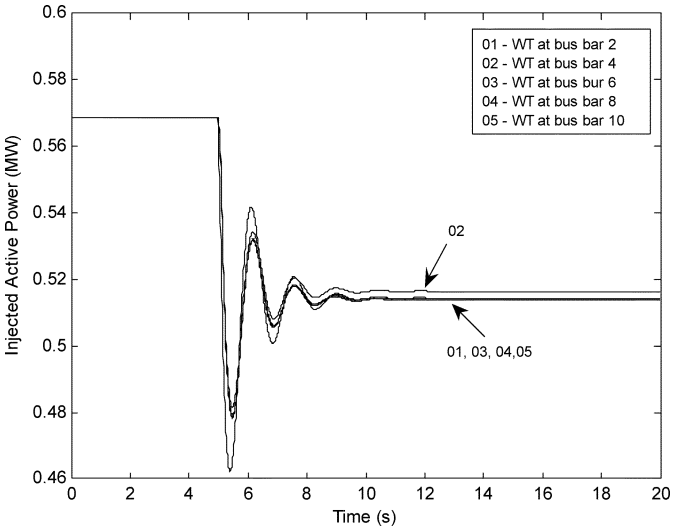

Fig. 7. Injected active power of each turbine for case *a*.

It was assumed that the system operator has requested to the SWFC for this wind farm to reduce its output to 2.5 MW and 1.0 MVAr. This was considered to happen 5 s after starting the simulation. This demands a total deloading of 12.28% regarding the total active power output delivery by the wind farm. For both cases *a* and *b*, Table II shows the new operating conditions of each WT after running the optimization procedure in the SWFC system.

In case *a*, all the wind turbines inject approximately the same active powers when active power losses are not considered in the optimization procedure, as can be seen from Table II and Fig. 7. The reduction of active power is initially performed by exploiting the available deloading in the DFIWG. In this way, the rotor speed increases when the active power is reduced, and as a consequence, the pitch angle is adjusted to a larger angle, aiming to reduce the mechanical power. The injected reactive power, the rotor speed, and pitch angle behaviors are shown in Figs. 8, 9, and 10, respectively.

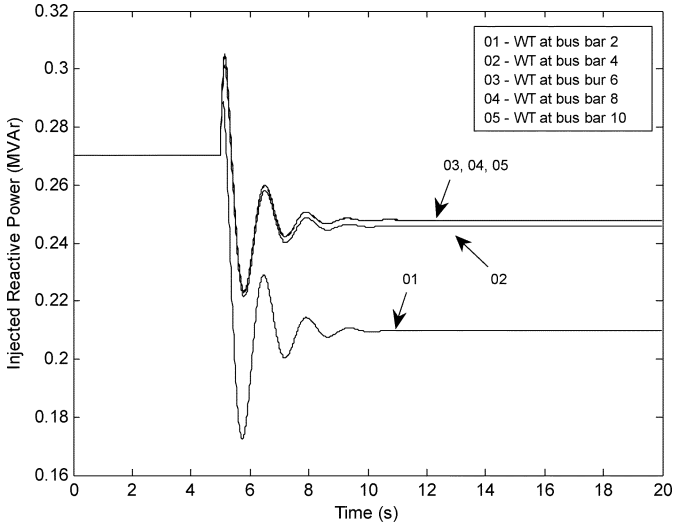

Fig. 8. Injected reactive power of each wind turbine for case *a*.

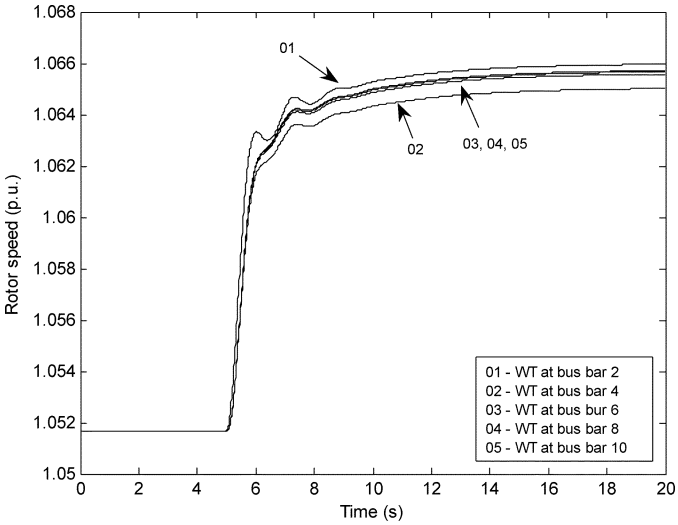

Fig. 9. Increasing of rotor speed referred to generator side due to decreasing of injected active power in case *a*.

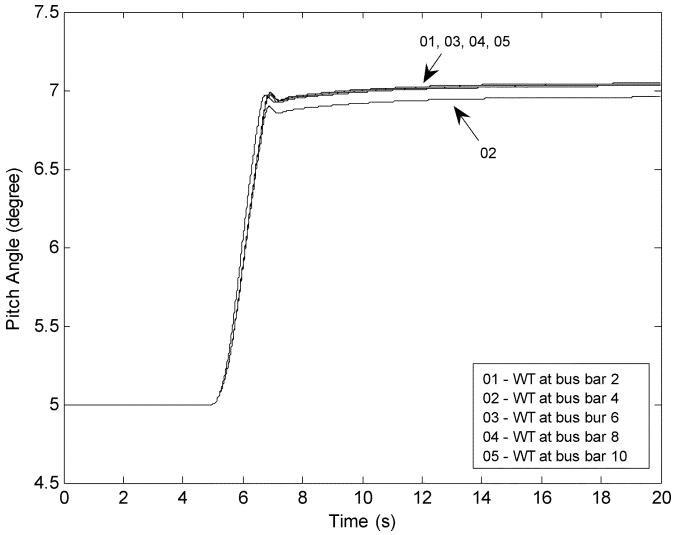

Fig. 10. Pitch angle for each WT for case *a*.

After running the optimization procedure, it is verified that more active and reactive powers are produced in case *a* than in

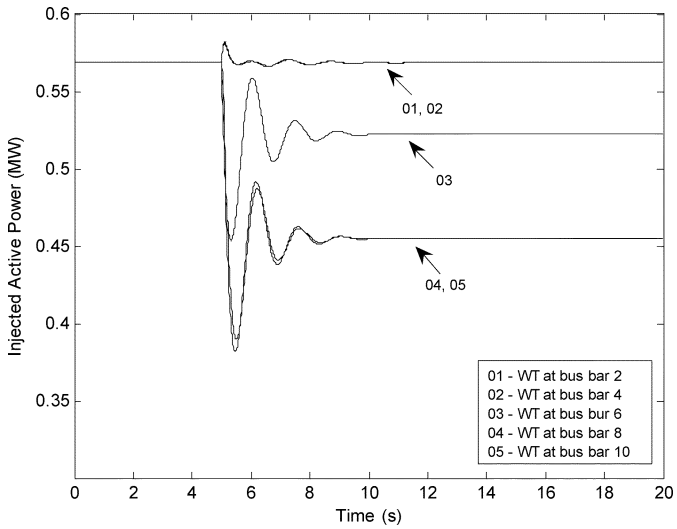

Fig. 11. Injected active power of each turbine for case *b*.

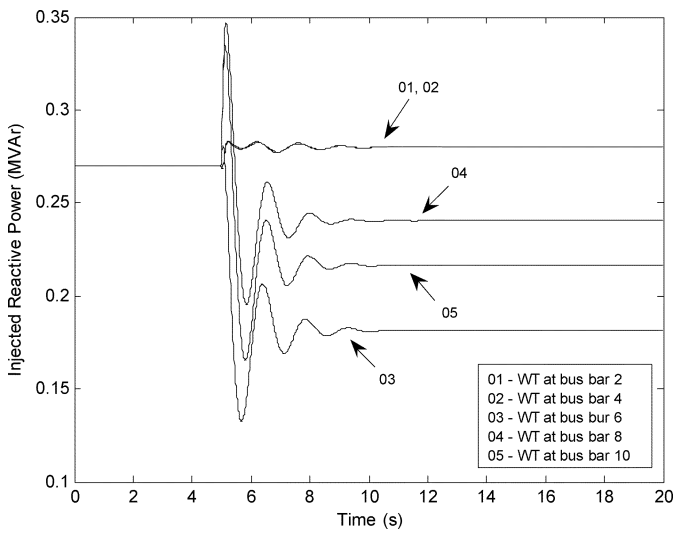

Fig. 12. Injected reactive power of each turbine for case *b*.

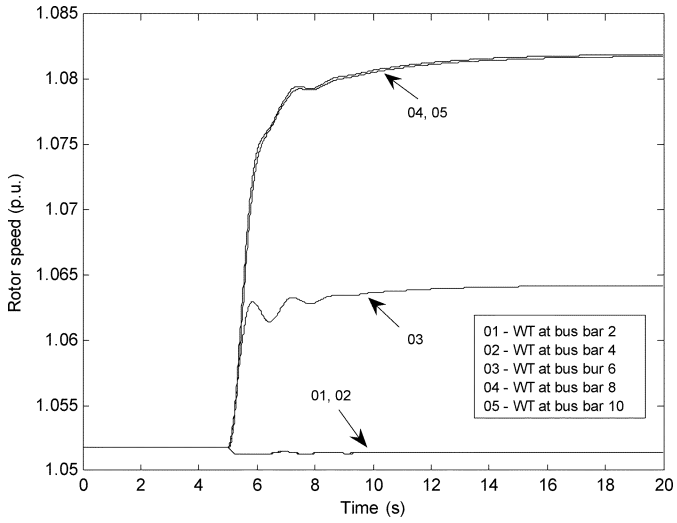

Fig. 13. Rotor speed referred to generator side of each WT for case *b*.

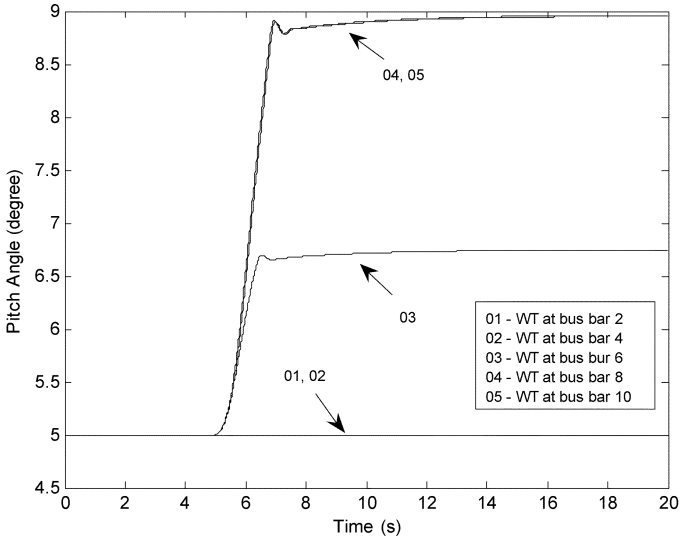

Fig. 14. Pitch angle of each WT for case *a*.

case *b* because in the first case, the active and reactive power losses just contribute to the reduction of the total mismatch of active and reactive powers delivery by wind farm to the grid. Two extreme situations should be mentioned for case *a*: 1) when more active power is required than is possible to deliver (considering the available wind power at the instant), the solution of problem is such that all WT will deliver the maximum available wind power; and 2) when the supervisor control requires a large reduction in the wind farm production, all the WT will generate their minimum value.

For case *b*, it can be observed that the more distant wind turbines from the grid connection point, namely, wind turbines connected at buses 8 and 10, respectively, reduce significantly their injected active power in order to decrease the active power losses. On the other hand, the closest WT from the connection point injects the maximum available active power. For this configuration, there is a decrease in active power losses of 1.71 kW regarding case *a*.

Nevertheless, once the reactive power losses are not considered in the optimization process, the injected reactive powers in both simulation cases for all WTs are adjusted accordingly, respecting the voltage restrictions and generator limits. However, due to the active power losses optimization concern, the closest WTs increase the injected reactive power (in this case, WTs at bus bar 2 and 4 operate with rated maximum reactive power), while the most distant WTs reduce the injected reactive power.

The dynamic behavior of active and reactive powers, as well as the rotor speed and pitch angles for all WT, are depicted in Figs. 11–14 for case *b*.

It must be stressed that, in case *b*, the weight factor regarding the deviation between wind farm generation and system operator request is more important $(p_1 = 1)$ than the weight factors affecting the reactive power deviation $(p_2 = 0.5)$ and loss reduction $(p_3 = 0.5)$. Therefore, the procedure only tackles losses minimization when the wind park active power output deviation becomes almost nil.

In general, case *a* presents the worst situation because it leads to larger losses than case *b*. Situations that consider different wind power availability levels would lead to similar results, with the closest WT tending to inject larger active and reactive powers according to a given wind speed and maximum rating limits.

The individual DFIWG control approach adopted proves to operate in a very effective manner, with the wind generators responding in a very fast way to the SWFC set-points.

IV. Conclusion

A soft wind farm active and reactive powers dispatch was developed in this paper to allow the optimization of the operation of large wind farms and or clusters of wind farms. This procedure is able to deal with internal wind grid loss minimization and with requests from system operators regarding limitation of wind parks generation output levels. Such a tool was developed to run at a SWFC level or to run at the Wind Power Dispatch Center. Further developments are needed in this optimization tool to be able to deal with the start and stop of wind generators in order to satisfy system operator requests related to large reductions in wind power generation levels.

The implementation of this optimized operation strategy was coupled with the introduction of a secondary active power control loop in doubly fed induction wind generators. These generators were operated under a deloaded optimal power extraction curve and controlled by pitch control and static converters, simultaneously. Large robustness of operation was achieved through the simultaneous adjustments provided by pitch control, allowing, in this way, wind turbines to operate permanently under optimal power curves with deloading capability characteristics that allow the machine to participate also in primary frequency control.

Appendix

A. Parameters

Base values for the per-unit system conversion.

Base Power: 100 MVA

Base Voltages: 0.69 kV for low-voltage bus-bar, 15 kV for medium-voltage bus-bar, and 63 kV for high voltage bus-bar.

B. Doubly Fed Induction Generator

P_n (kW) $= 660$, V_n (V) $= 690$, R_s (p.u.) $= 0.067$, X_s (p.u.) $= 0.03$, R_r (p.u.) $= 0.0058$, X_r (p.u.) $= 0.0506$, X_m (p.u.) $= 2.3161$, ω_s (r.p.m) $= 1500$, No. of poles $= 4$, rated slip generator $= 2\%$, dc voltage $= 326.60$ V, capacitor $= 284\ \mu$F.

C. Wind Turbine

No. of blades $= 3$, Rotor diameter $= 22$ m, cut-in speed $= 4$ m/s, cut-off speed $= 25$ m/s, Atm. density $= 1.225$ Kg.m^{-3}, Inertia time constant $= 4$, Gear box ratio 1: 45

D. Transformers

Wind generator rotor transformer (200:690 V): S_n (kVA) $= 100$, reactance $= 9.5\%$; wind generator stator transformer (0.69:15 kV): S_n (kVA) $= 750$, reactance $= 5\%$; Wind farm transformer (15:63 kV): S_n (MVA) $= 3.75$, reactance $= 5\%$.

References

[1] V. Akhmatov, "Analysis of dynamic behavior of electric power system with large amount of wind power," Ph.D. dissertation, Elect. Power Eng., Ørsted-DTU, Technical Univ. Denmark, Lyngby, Denmark, Apr. 2003.

[2] J. G. Slootweg, S. W. H. de Haan, H. Polinder, and W. L. Kling, "Modeling wind turbine in power system dynamics simulations," in *Proc. IEEE Power Engineering Society Summer Meeting*, Vancouver, BC, Canada, Jul. 2001, pp. 15–19.

[3] R. Pena, J. C. Clare, and G. M. Asher, "Doubly fed induction generator using back-to-back PWM converters and its applications to variable-speed wind-energy generation," *Proc. Inst. Elect. Eng., Elect. Power Appl.*, vol. 143, no. 3, pp. 231–241, May 1996.

[4] J. Ekanayake and N. Jenkins, "Comparison of the response of doubly fed and fixed-speed induction generator wind turbines to changes in network frequency," *IEEE Trans. Energy Convers.*, vol. 19, no. 4, pp. 800–802, Dec. 2004.

[5] J. Ekanayake, L. Holdsworth, and N. Jenkins, "Control of DFIG wind turbines," *Power Eng. J.*, vol. 17, no. 1, pp. 28–32, Feb. 2003.

[6] M. V. A. Nunes *et al.*, "Influence of the variable-speed wind generators in transient stability margin of the conventional generators integrated in electrical grids," *IEEE Trans. Energy Convers.*, vol. 19, no. 4, pp. 692–701, Dec. 2004.

[7] R. G. de Almeida, J. A. Peças Lopes, and J. A. L. Barreiros, "Improving power system dynamic behavior through doubly fed induction machines controlled by static converter using fuzzy control," *IEEE Trans. Power Syst.*, vol. 19, no. 4, pp. 1942–1950, Nov. 2004.

[8] J. L. Rodriguez-Amenedo *et al.*, "Automatic generation control of a wind farm with variable speed wind turbines," *IEEE Trans. Energy Convers.*, vol. 17, no. 2, pp. 279–284, Jun. 2002.

[9] P. Kundur, *Power System Stability and Control*. New York: McGraw-Hill, 1994.

[10] E. D. Castronuovo, J. M. Campagnolo, and R. Salgado, "New versions of nonlinear interior point methods applied to the optimal power flow," in *Proc. IEEE T&D Latin America*, São Paulo, Brazil, Apr. 2002.

[11] H. Akagi *et al.*, "Instantaneous reactive power compensators comprising switching devices without energy storage components," *IEEE Trans. Ind. Appl.*, vol. IA-20, pp. 625–630, May/Jun. 1984.

Rogério G. de Almeida received the B.Sc. and M.Sc. degrees from the Federal University of Pará, Belem, Brazil, in 1996 and 1999, respectively. He is currently working toward the Ph.D. degree, concentrating on the effects of large technology on power system dynamics, namely, renewable energy generation. The research is carried out at the Power System Unit, Instituto de Engenharia de Sistemas e Computadores do Porto (INESC), Porto, Portugal.

His main interests are focused on power system dynamic analysis, electrical machines, and power electronics.

Edgardo D. Castronuovo (M'03) received the B.Sc. degree in electrical engineering in 1995 from the National University of La Plata, Argentina, the M.Sc. and Ph.D. degrees from the Federal University of Santa Catarina, Brazil, in 1997 and 2001, respectively, and performed postdoctoral work in 2005 at Instituto de Engenharia de Sistemas e Computadores do Porto (INESC), Porto, Portugal.

He worked in the power system areas at CEPEL, Brazil, and INESC.

J. A. Peças Lopes (M'80–SM'94) received the Electrical Engineering degree (five-year course), the Ph.D. degree in electrical engineering, and the Aggregation degree from the University of Porto, Porto, Portugal, in 1981, 1988, and 1996, respectively.

He is an Associate Professor of aggregation with the Department of Electrical Engineering, Faculty of Engineering, University of Porto. In 1989, he joined the staff of Instituto de Engenharia de Sistemas e Computadores do Porto (INESC) as a Senior Researcher, and he is presently Co-coordinator of the Power Systems Unit of INESC.